

Doxorubicin-peptide-gold nanoparticle conjugate as a functionalized drug delivery system: exploring the limits

Kai S. Exner^{1,2}, Anela Ivanova^{1,*}

¹*Sofia University, Faculty of Chemistry and Pharmacy, Department of Physical Chemistry,
1 James Bourchier blvd., 1164 Sofia, Bulgaria*

²*Cluster of Excellence RESOLV, Bochum, Germany*

* Corresponding author: aivanova@chem.uni-sofia.bg

ORCID: 0000-0003-2934-6075 (KSE); 0000-0001-6220-7961 (AI)

Electronic Supplementary Information (ESI)

1 Investigated model NP-DBP-2DOX

The drug-delivery system (DDS) component modeled in this study consists of a methyl thiolate-protected gold nanoparticle (Au-NP), a drug-binding peptide (DBP), and two doxorubicin (DOX) entities in saline. An illustration of the model of the associate NP-DBP-2DOX in a periodic box is shown in **Figure S1**.

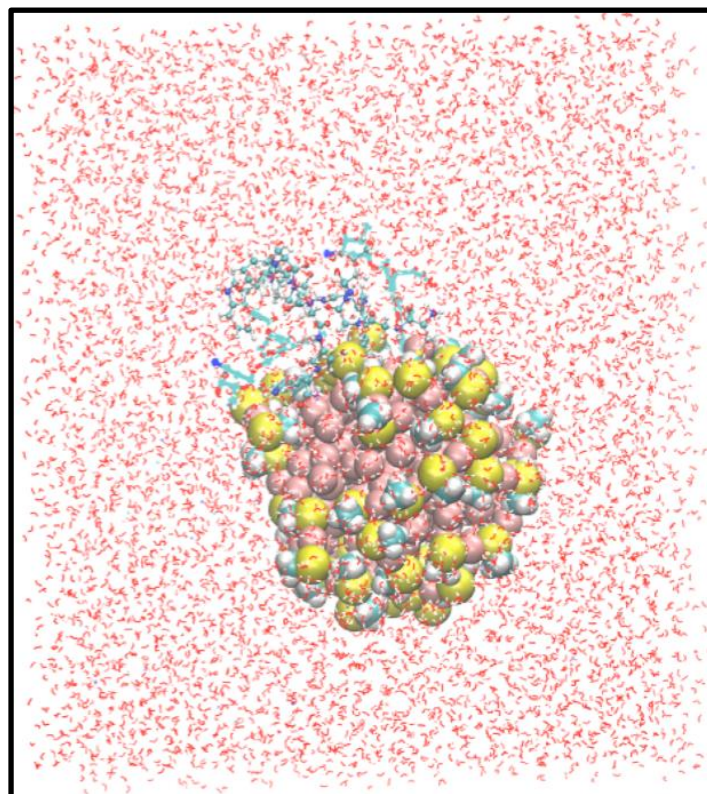


Figure S1. Full snapshot of the NP-DBP-2DOX conjugate in a periodic box, modeled by a combination of molecular dynamics simulations and density functional theory calculations. The Au-NP is sketched with vdW spheres, lines are used for DOX and water, and all amino acids of the DBP are in CPK representation.

Equilibration of the associate NP-DBP-2DOX is verified by the evolution of the total energy, temperature, pressure, and the root-mean-square deviation (RMSD) of the atomic coordinates of the highly flexible DBP with respect to the coordinates of the minimized structure. A summary is given in **Figure S2**, while the average values are collected in **Table S1**.

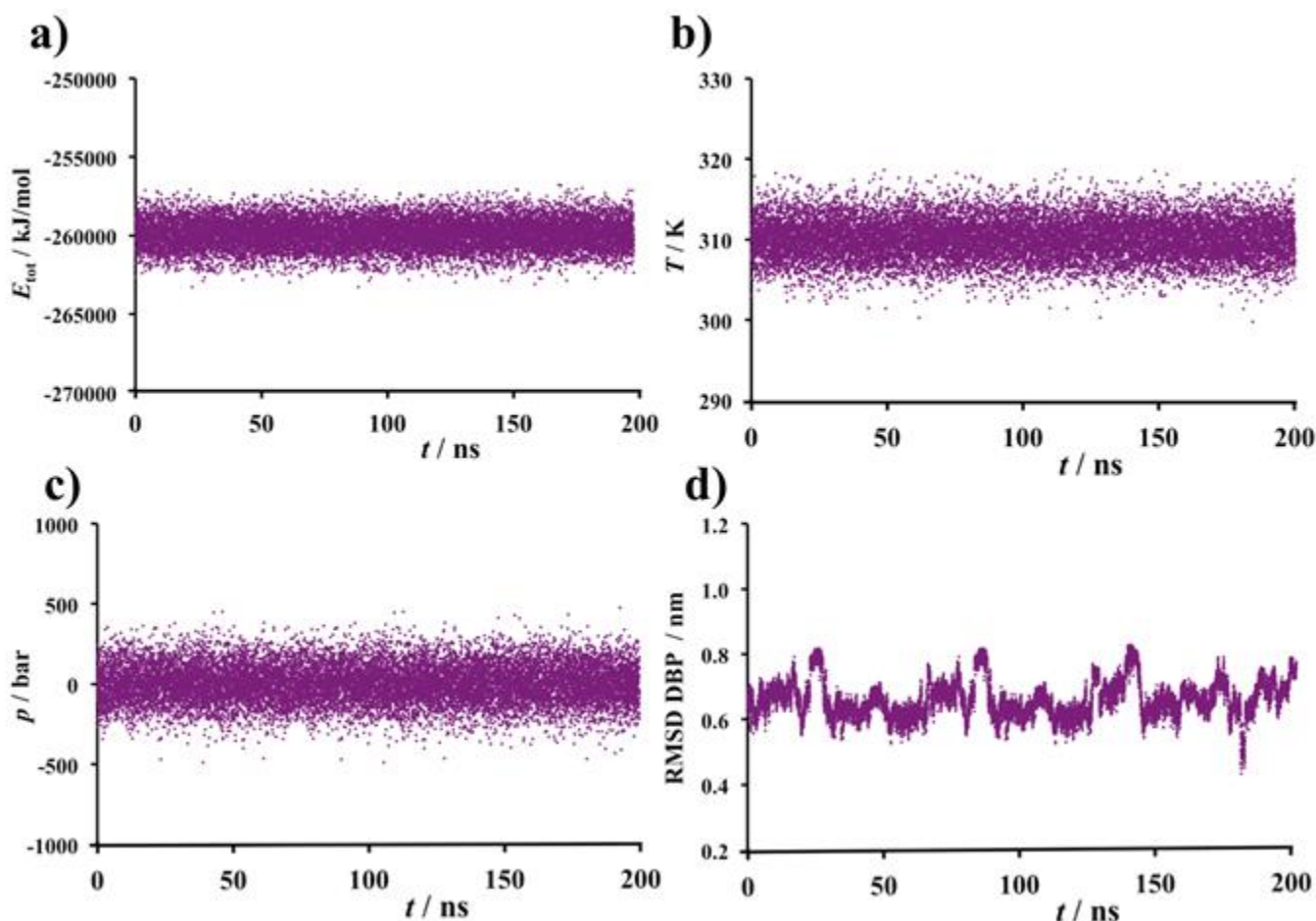


Figure S2. a) Total energy, b) temperature, c) pressure, and d) RMSD of the DBP in the associate NP-DBP-2DOX during the production phase.

Table S1. Average values and standard deviations of total energy, temperature, and pressure for the associate NP-DBP-2DOX within the production phase (200 ns).

System	E_{tot} / kJ/mol	T / K	p / bar
NP-DBP-2DOX	-259906 ± 921	310.0 ± 2.5	1.0 ± 119.6

To allow comparison of the NP-DBP-2DOX complex with the associate NP-DBP-DOX, modeled in our previous study,^[S1] we calculate the Au-Au radial distribution function (RDF) to assess the structure of the Au-NP carrier moiety. **Figure S3** depicts the RDF for both systems.

Two peaks at $r_1 = 0.33$ nm and $r_2 = 0.66$ nm are visible for the associate NP-DBP-DOX, while the presence of the second drug molecule shifts these peaks slightly to the right ($r_1 = 0.35$ nm and $r_2 = 0.69$ nm). This indicates an increase in NP size, which is verified by evaluating the effective size of the Au-NP from the RDF, taking $g(r) < 2$ as cut-off condition. We obtain nanoparticle diameters of 2.23 nm and 2.46 nm in the systems NP-DBP-DOX and NP-DBP-2DOX, respectively. Thus, the diameter of the Au-NP becomes larger by about 10 % as soon as a second drug molecule is carried by the associate NP-DBP, corresponding to an increase in the NP surface area of about 20 %. We mainly trace the increase in NP

size to the fact that the peptide is more spread on the surface of the Au-NP when two drug molecules are transported by the DDS component. Consequently, the Au atoms relocate in order to allow sufficient interaction of the NP caps with both the peptide and the drug entities, indispensably requiring a larger surface area to cope with all residues. The surge in NP size compared to the NP-DBP-DOX conjugate is further corroborated by an increase in the radius of gyration (R_G) and a larger solvent accessible surface area (SASA), while the analysis of the moments of inertia along the three principal axes reveals a deformed-sphere-like behavior of the Au-NP within the NP-DBP-2DOX associate. **Figure S4** and **Table S2** summarize the data and provide statistics, respectively.

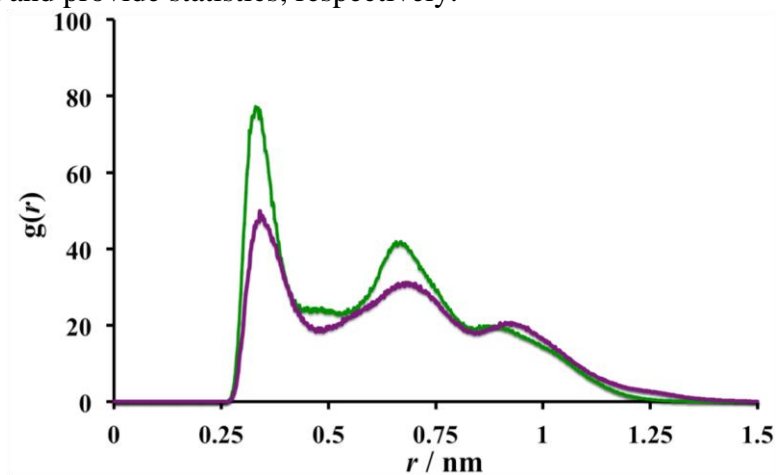


Figure S3. Au-Au radial distribution functions of the associates NP-DBP-DOX^[S1] (green) and NP-DBP-2DOX (violet).

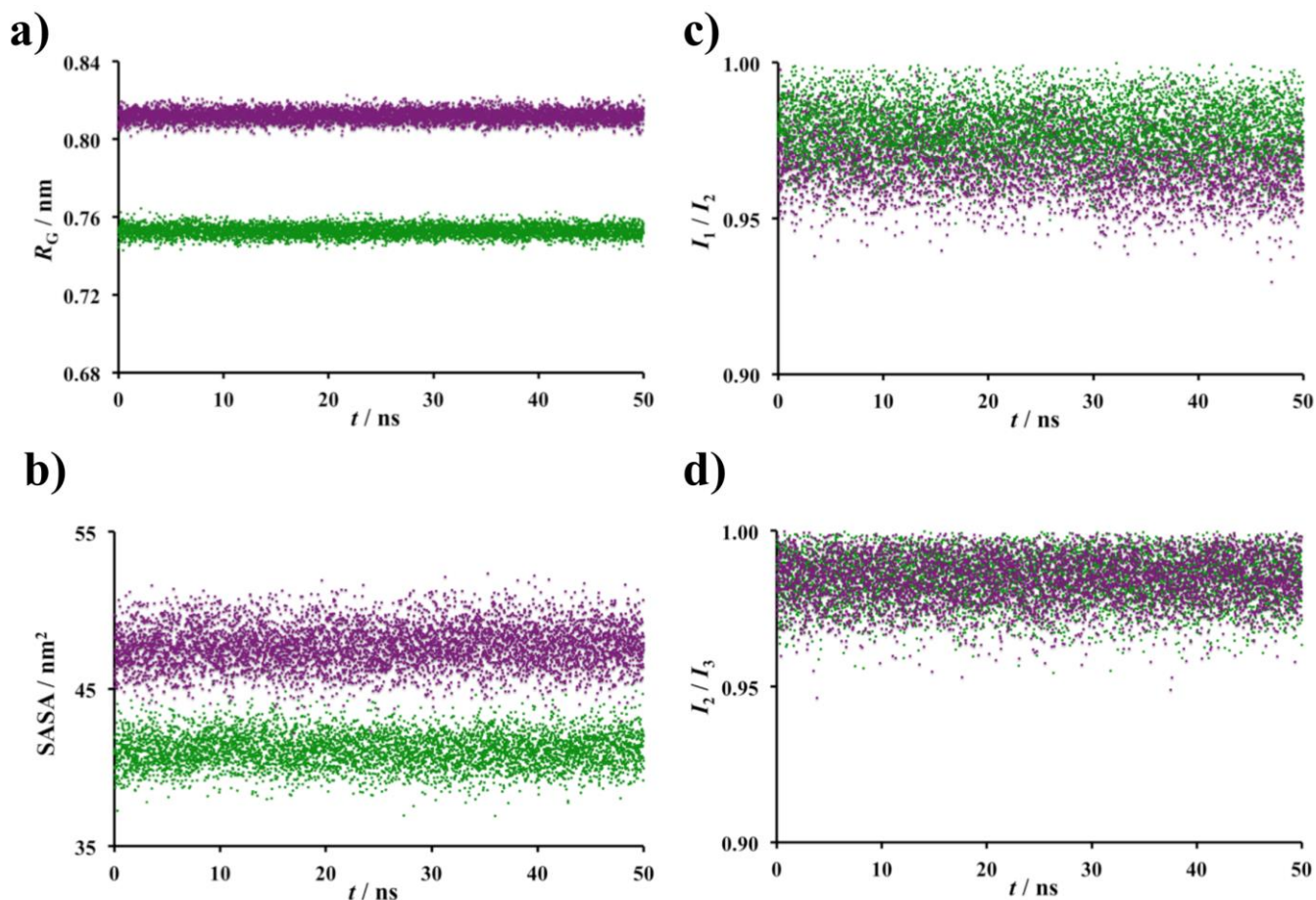


Figure S4. **a)** Radius of gyration (R_G) of the Au₁₁₄ core, **b)** solvent accessible surface area (SASA), and ratios of the moments of inertia **c)** I_1/I_2 and **d)** I_2/I_3 for the complexes NP-DBP-DOX^[S1] (green) and NP-DBP-2DOX (violet).

Table S2. Average values and standard deviations of the radius of gyration (R_G), the SASA, and the ratios I_1/I_2 and I_2/I_3 for the associates NP-DBP-DOX and NP-DBP-2DOX, estimated from the first 50 ns of the product phase trajectories. The data of the NP-DBP-DOX conjugate are taken from our previous work.^[S1]

System	R_G / nm	SASA / nm ²	I_1/I_2	I_2/I_3
NP-DBP-DOX	0.753 ± 0.003	41.1 ± 1.1	0.979 ± 0.009	0.984 ± 0.008
NP-DBP-2DOX	0.812 ± 0.005	47.8 ± 1.6	0.959 ± 0.012	0.982 ± 0.009

For NP-DBP-2DOX, the ratios I_1/I_2 and I_2/I_3 amount to 0.959 and 0.982 on average. Thus, due to $I_1/I_2 < I_2/I_3$, we observe a deformed-sphere behavior of the Au-NP, that is, the NP is not an ideal sphere anymore, but somewhat elongated in the direction where the DBP and the drug molecules interact with the caps of the NP.

The SASA rises from 41.1 nm² for the associate NP-DBP-DOX to 47.8 nm² for NP-DBP-2DOX, corresponding to an increase of about 16 %. This coincides qualitatively with the enlarged surface area of about 20 %, as quantified by analyzing the RDF (**Figure S3**) or the radius of gyration (**Figure S4a**). Actually, the average values indicate that the radius of gyration is about 8 % larger for NP-DBP-2DOX compared to NP-DBP-DOX, giving rise to a quantitative agreement between the increase in NP size and the enlarged solvent accessible surface area.

In conclusion, the presence of a second DOX molecule in the DDS component affects the structural characteristics of the Au-NP, resulting in an elongated, non-spherical NP due to the additional drug entity. Besides, a different behavior of the drug molecules compared to the associate NP-DBP-DOX, discussed in our previous study,^[S1] is witnessed. We focus on the surface chemistry of the two DOX entities in the main text of the manuscript (Section 3).

2 Adsorption configurations in the associate NP-DBP-2DOX

In Section 3 of the main text, we summarize the observed adsorption structures of the two drug molecules DOX₁ and DOX₂ as well as their existence times within the 200 ns production trajectory (**Figure 2** and **Figure 3**). In this Section, the respective configurations are depicted with enlarged resolution.

Figure S5 shows adsorption configuration **a**), in which DOX₁ is intercalated between the caps of the NP and the tryptophan residue W5, while DOX₂ is intercalated between the caps of the NP and W8.

Figure S6 shows adsorption configuration **b**), in which DOX₁ is intercalated between the caps of the NP and W5, while DOX₂ is non-specifically intercalated between the caps of the NP and the backbone of the peptide, that is, there is no specific interaction of DOX₂ with any amino acid from the DBP.

Figure S7 shows adsorption configuration **c**), in which DOX₁ is stacked by W5 in a perpendicular arrangement to the NP surface, where part of the anthracycline fragment of DOX₁ interacts with the caps of the NP. DOX₂ is non-specifically intercalated between the caps of the NP and the peptide backbone.

Figure S8 shows adsorption configuration **d**), in which DOX₁ is stacked by W5 in a perpendicular arrangement to the NP surface, while DOX₂ is intercalated between W8 and W13.

Figure S9 shows adsorption configuration **e**), in which DOX₁ is stacked by W5 in a perpendicular arrangement to the NP surface, while DOX₂ is intercalated between the tyrosine residue Y9 and the caps of the NP.

Figure S10 shows a snapshot of the trajectory at $t = 200$ ns, indicating that DOX₁ is bound to the DDS component, whereas DOX₂ has dissociated into the saline solution.

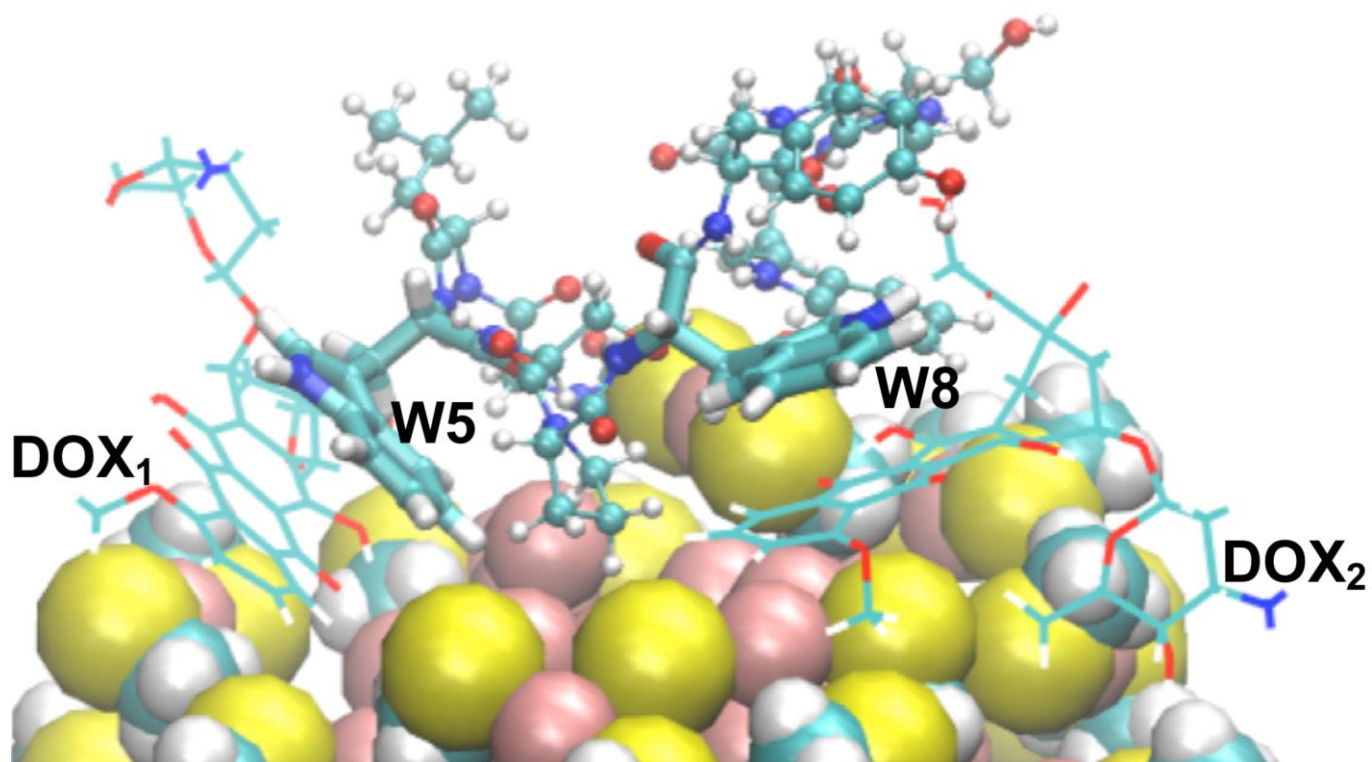


Figure S5. Enlarged depiction of **Figure 2a** from the main text. The Au-NP is sketched with vdW spheres and lines are used for DOX. Tryptophan or tyrosine residues of the DBP that directly interact with any of the two DOX entities are highlighted with licorice, whereas all other amino acids of the DBP are in CPK representation. The interacting partners of the DBP and the two DOX entities are labeled.

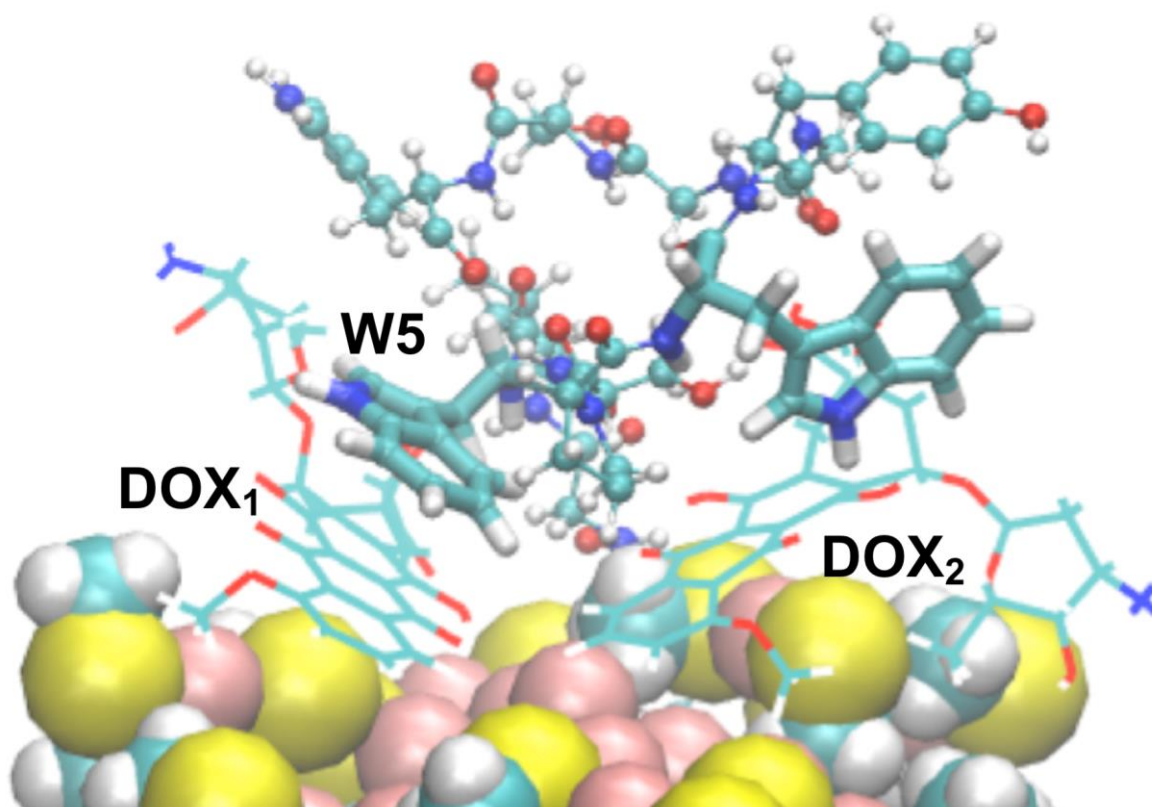


Figure S6. Enlarged depiction of **Figure 2b** from the main text. The Au-NP is sketched with vdW spheres and lines are used for DOX. Tryptophan or tyrosine residues of the DBP that directly interact with any of the two DOX entities are highlighted with licorice, whereas all other amino acids of the DBP are in CPK representation. The interacting partners of the DBP and the two DOX entities are labeled.

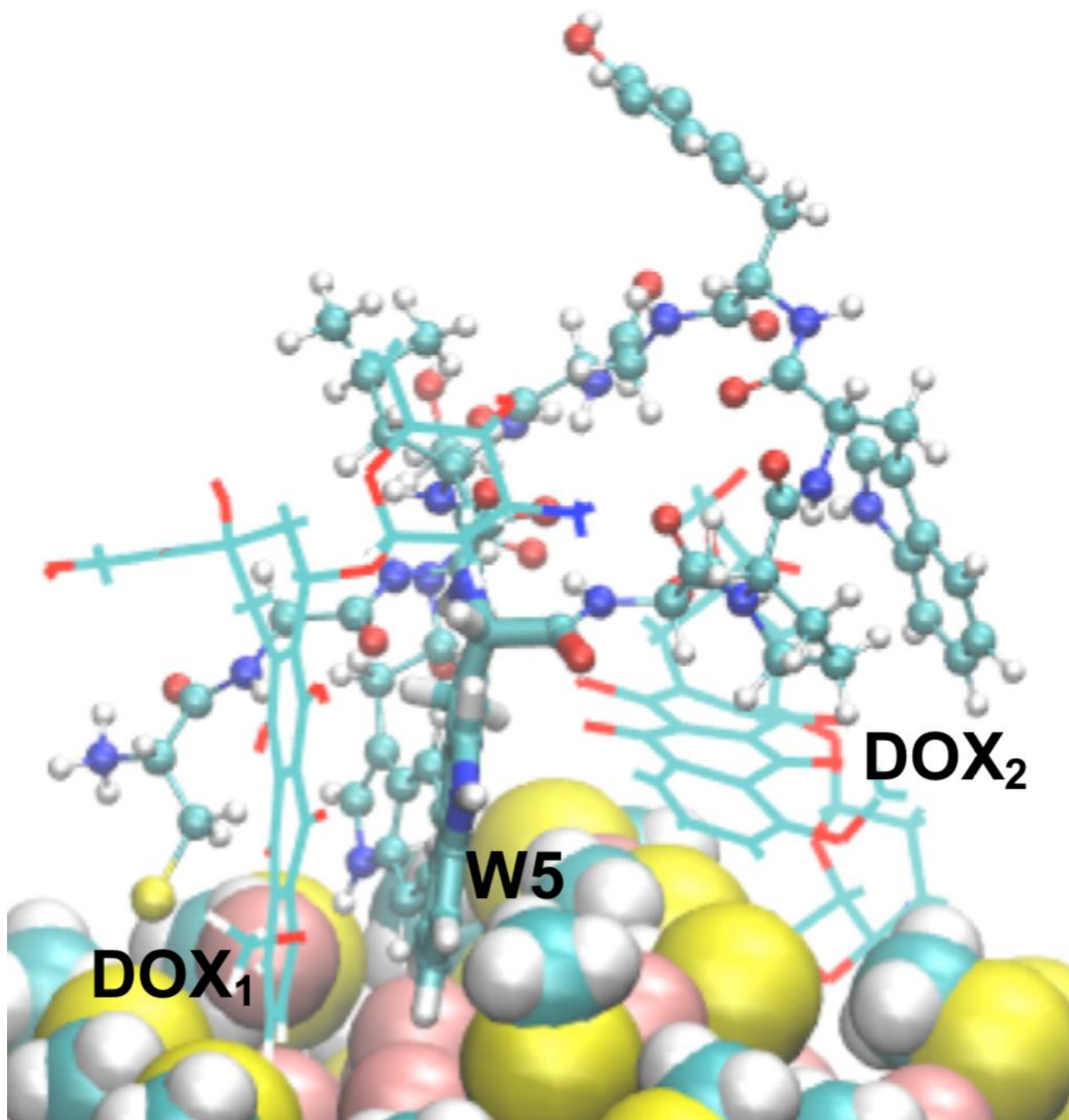


Figure S7. Enlarged depiction of **Figure 2c** from the main text. The Au-NP is sketched with vdW spheres and lines are used for DOX. Tryptophan or tyrosine residues of the DBP that directly interact with any of the two DOX entities are highlighted with licorice, whereas all other amino acids of the DBP are in CPK representation. The interacting partners of the DBP and the two DOX entities are labeled.

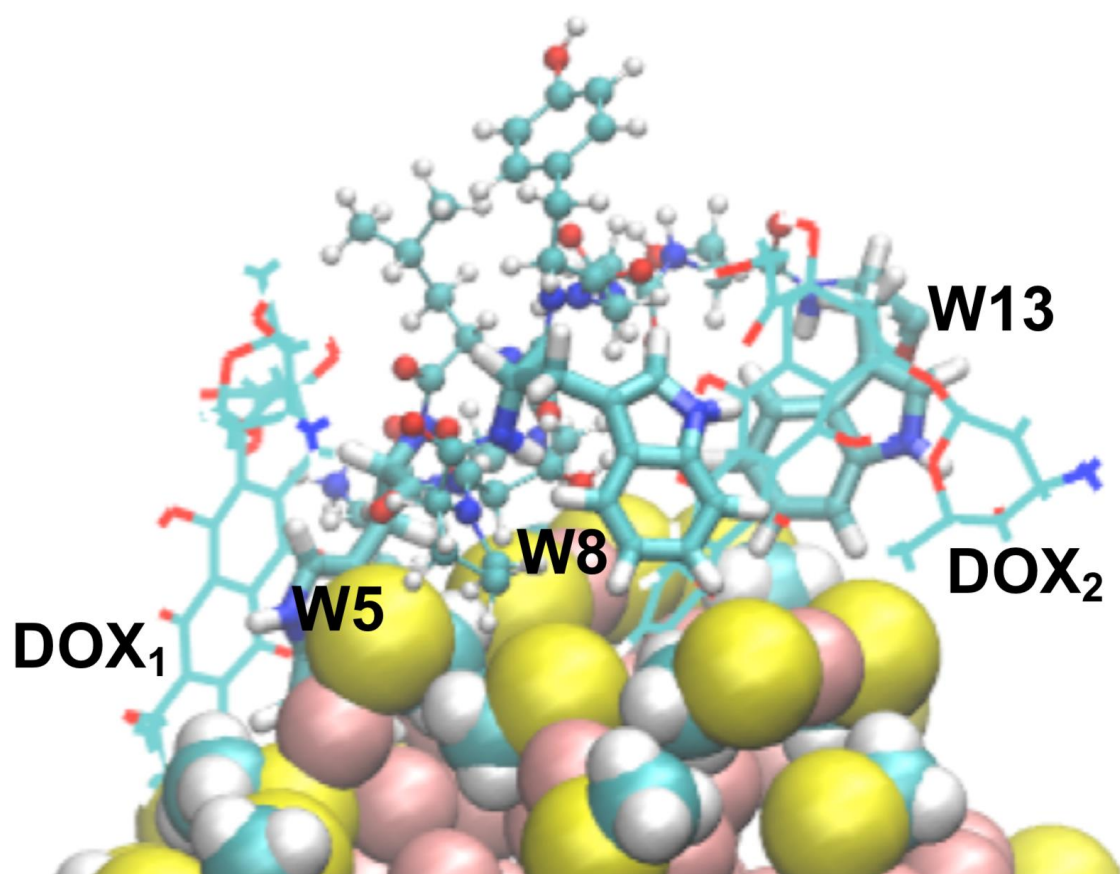


Figure S8. Enlarged depiction of **Figure 2d** from the main text. The Au-NP is sketched with vdW spheres and lines are used for DOX. Tryptophan or tyrosine residues of the DBP that directly interact with any of the two DOX entities are highlighted with licorice, whereas all other amino acids of the DBP are in CPK representation. The interacting partners of the DBP and the two DOX entities are labeled.

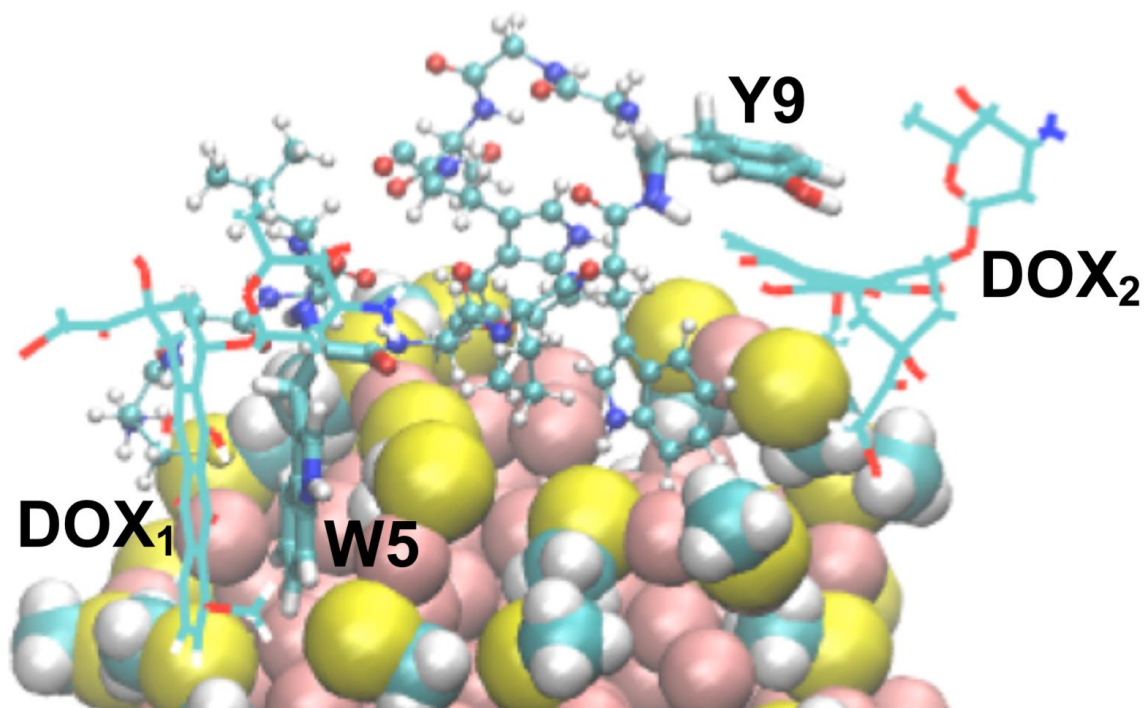


Figure S9. Enlarged depiction of **Figure 2e** from the main text. The Au-NP is sketched with vdW spheres and lines are used for DOX. Tryptophan or tyrosine residues of the DBP that directly interact with any of the two DOX entities are highlighted with licorice, whereas all other amino acids of the DBP are in CPK representation. The interacting partners of the DBP and the two DOX entities are labeled.

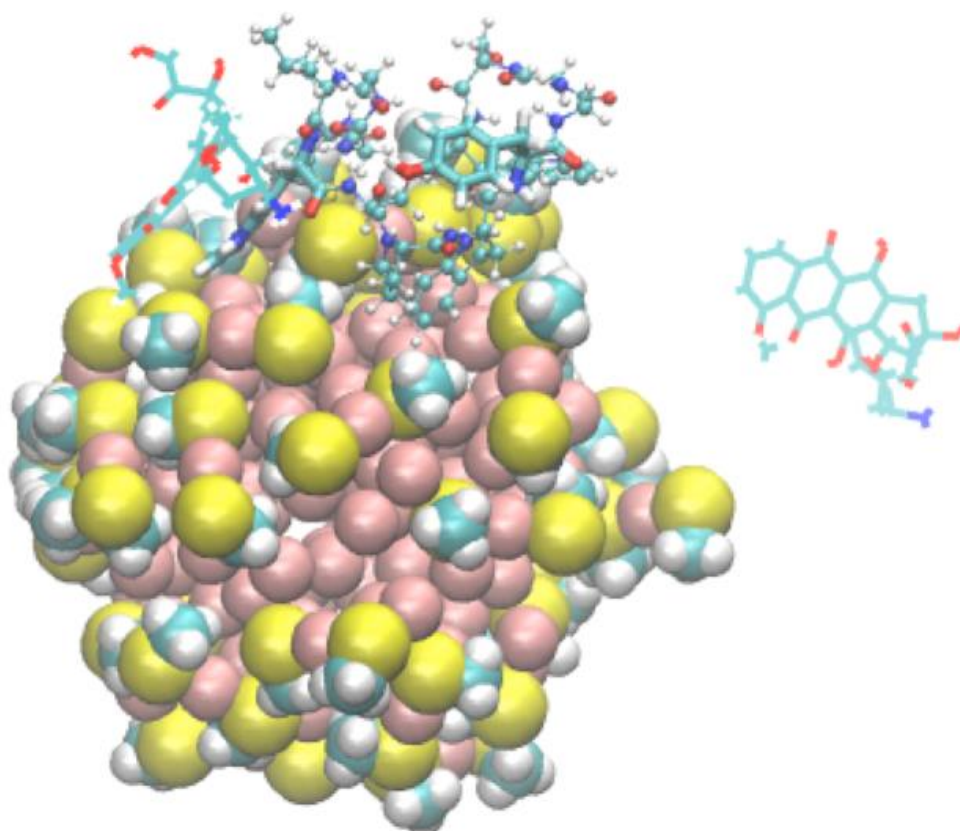


Figure S10. Snapshot of the trajectory at $t = 200$ ns. While DOX₁ (left-hand side) is stabilized by the DDS component, DOX₂ (right-hand side) has dissociated into the saline solution. Water molecules and inorganic ions are omitted for clarity. The Au-NP is sketched with vdW spheres and lines are used for DOX. Tryptophan or tyrosine residues of the DBP that directly interact with any of the two DOX entities are highlighted with licorice, whereas all other amino acids of the DBP are in CPK representation.

3 Analysis of the MD trajectories

In the initial configuration of the associate NP-DBP-2DOX, DOX₁ is interacting with the caps of the Au-NP and the tryptophan residue W5, as observed in our previous study for the conjugate NP-DBP-DOX.^[S1] DOX₂ is placed randomly in the saline solution surrounding the NP-DBP-DOX complex. Already during relaxation of the entire system, DOX₂ also adsorbs on the NP-DBP carrier, finding the tryptophan residue W8 in conjunction with the caps of the Au-NP as a stable adsorption site. The different adsorption configurations of both drug entities, as observed in the 200 ns production phase of the MD trajectory, are summarized in **Figure S5 – S10**. In the following, we discuss the surface chemistry of both drug molecules.

Relating to DOX₁, we can distinguish two different adsorption states. While for $0 \text{ ns} < t < 85 \text{ ns}$ DOX₁ is intercalated between the caps of the NP and W5 (**Figure S5 – S6**), for $85 \text{ ns} < t < 200 \text{ ns}$ DOX₁ is stacked by W5 in a perpendicular orientation to the NP surface (**Figure S7 – S9**), thereby maintaining its interaction with the caps of the carrier moiety. **Figure S11a** depicts the evaluated distances of the center of masses (COMs) of the anthracycline fragment of DOX₁ and the indole residue of W5 for the production-phase trajectory. In **Figure S11b-c** the minimum distance of DOX₁ to the caps as well as the

number of contacts between DOX₁ and the caps are plotted. Average data for the two competing adsorption configurations are summarized in **Table S3**.

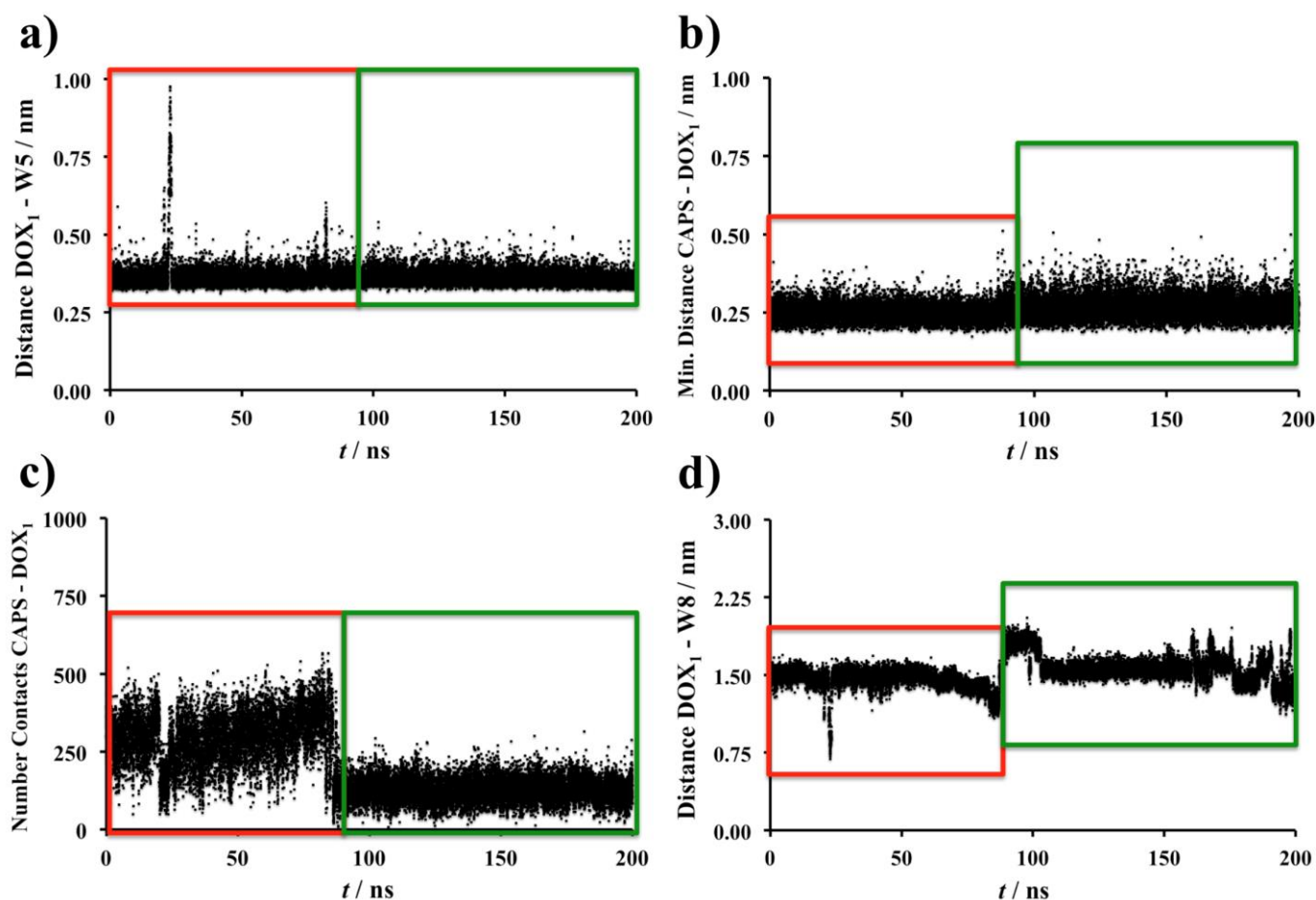


Figure S11. **a)** Distance between the COMs of the indole of W5 and the anthracycline part of DOX₁; **b)** minimum distance between the methyl thiolate caps and DOX₁; **c)** number of contacts between the methyl thiolate caps of the Au-NP and DOX₁; **d)** distance between the COMs of the indole of W8 and the anthracycline part of DOX₁. Red boxes mark the CAPS–DOX₁–W5 sandwich structure (**Figure S5-S6**), green boxes indicate the W5–DOX₁ adsorption configuration perpendicular to the NP surface (**Figure S7-S9**).

Table S3. Average values and standard deviations of the distances W5–DOX₁ and W8–DOX₁, minimum distance between the methyl thiolate caps and DOX₁, and number of contacts between the methyl thiolate caps and DOX₁; separate estimates are compiled for the CAPS–DOX₁–W5 and W5–DOX₁ configurations.

Adsorption configuration	CAPS–DOX ₁ –W5	W5–DOX ₁
Distance (W5–DOX ₁) / nm	0.37 ± 0.05	0.37 ± 0.03
Minimum Distance (CAPS–DOX ₁) / nm	0.25 ± 0.03	0.27 ± 0.04
Number of Contacts (CAPS–DOX ₁)	294 ± 83	130 ± 45
Distance (W8–DOX ₁) / nm	1.46 ± 0.09	1.57 ± 0.14

Figure S11a reveals that the W5–DOX₁ distance remains virtually constant (about 0.37 nm), independent of the switch in adsorption configuration. The same finding also refers to the minimum distance of DOX₁ to the caps (**Figure S11b**). There, the standard deviation slightly increases in the perpendicular adsorption configuration (W5–DOX₁) compared to the sandwich state (CAPS–DOX₁–W5) (**Table S3**). Both observations differ from the behavior of the drug in the conjugate NP-DBP-DOX.^[S1] In the DDS component with one DOX entity, the W5–DOX distance was smaller (0.37 nm vs. 0.61 nm) and

the minimum distance of DOX to the caps was larger (0.52 nm *vs.* 0.25 nm) in the perpendicular adsorption configuration compared to the sandwich state. This indicates that W5 never moves apart from DOX₁ in the associate NP-DBP-2DOX, which contributes to the spreading of the peptide over the NP surface, accompanied with straining the DBP structure (cf. main text, Section 3).

The number of contacts between DOX₁ and the caps decreases as soon as DOX₁ changes from the sandwich state to the perpendicular adsorption configuration (**Figure S11c**). This observation is in line with the results for the conjugate NP-DBP-DOX^[S1] and can be explained by the fact that in the perpendicular adsorption configuration only part of the anthracycline fragments can interact with the caps, whereas in the sandwich state the entire anthracycline part is in direct proximity to the surface of the NP.

In our previous study addressing the conjugate NP-DBP-DOX, we observed that the adsorption configuration of DOX is coupled to the location of the tryptophan residue W8 in the peptide.^[1] **Figure S11d** depicts the COM-COM distance of W8 to DOX₁ as a function of time. A similar picture compared to the conjugate NP-DBP-DOX is also encountered for the associate NP-DBP-2DOX, as the W8–DOX₁ distance noticeably increases as soon as DOX₁ switches from the sandwich to the perpendicular adsorption state (**Table S3**).

In contrast to DOX₁, the surface chemistry of DOX₂ is somewhat more complicated since DOX₂ changes more often its interaction partners within the DDS component. While for 0 ns < *t* < 70 ns DOX₂ is intercalated between the caps of the NP and W8 (**Figure S5**), after 70 ns DOX₂ leaves its tryptophan interaction partner. Instead of searching for another tryptophan residue in the DBP, DOX₂ intercalates non-specifically between the caps of the NP and the backbone of the peptide (70 ns < *t* < 185 ns; **Figure S6-S7**). Thereafter, DOX₂ explores different adsorption sites on the surface of NP-DBP, moving from an intercalation complex with the tryptophan residues W8 and W13 (185 ns < *t* < 190 ns; **Figure S8**) to another intercalation configuration with the tyrosine entity W9 and the caps of the NP (190 ns < *t* < 195 ns; **Figure S9**). As discussed in Section 3 of the main text, the interaction of DOX₂ with the peptide is repulsive in the latter two adsorption states (main text, **Table 2**), resulting in the spontaneous release of the drug from the DDS component (195 ns < *t* < 200 ns; **Figure S10**).

Figure S12a depicts the evaluated distances, referring to the COMs of the anthracycline fragment of DOX₂ and the indole residue of W8 for the production phase. In **Figure S12b-c**, the minimum distance of DOX₂ to the caps as well as the number of contacts between DOX₂ and the caps are compiled. Statistical averaging of the data for the competing adsorption configurations is given in **Table S4**.

Figure S12a indicates that the distance W8–DOX₂ significantly increases after 70 ns, which coincides with the switch in adsorption configuration from the sandwich state (CAPS–DOX₂–W8) to the non-specific intercalation between the caps and the peptide backbone. Since DOX₂ maintains its location in direct proximity to the caps, the minimum distance of DOX₂ to the caps as well as the number of contacts between DOX₂ and the caps are nearly unaffected by the change in adsorption configuration (**Table S4**).

However, so far, it cannot be understood why DOX₂ leaves its stacking partner W8 to intercalate non-specifically between the caps of the Au-NP and the backbone of the peptide. Previous studies of Gocheva et al. for the conjugate DBP-DOX without the NP showed that dimer formation of two DOX residues is energetically favorable,^[S2] albeit dimer formation between two DOX entities is not observed in this study. **Figure S12d** depicts the COM-COM distance of DOX₁ to DOX₂ as a function of time. As soon as DOX₂ moves off its stacking partner W8 (*t* = 70 ns), DOX₂ significantly reduces its distance to DOX₁. This may indicate that DOX₂ is searching for proximity to DOX₁, which, in the optimum case, could result in the formation of a DOX-DOX dimer. Since DOX₁ is trapped in the sandwich state CAPS–DOX₁–W5, dimer formation cannot occur due to steric reasons. On the other hand, DOX₁ changes its

adsorption configuration from the sandwich state to the perpendicular adsorption configuration W5–DOX₁ at $t = 85$ ns (**Figure S11**). In this state, the tryptophan residue W5 serves as a protection shield for DOX₁, making dimer formation between the two drug molecules unfeasible (**Figure S7**).

In conclusion, considering the fact that DOX₂ forsakes an energetically well-stabilized sandwich complex with the tryptophan residue W8 and moves toward DOX₁, this may indicate that there is a driving force of DOX₂ to form a DOX-DOX dimer. The presence of the Au-NP in the DDS component, though, increases the degrees of freedom of the system, and since both drug entities heavily interact with the NP (**Table S3-S4**), dimer formation does not take place. In this case, at least one drug residue would need to leave the surface of the NP, thereby losing an attractive interaction partner (cf. main text, **Table 1**); this may corroborate why dimer formation is not observed for the conjugate DBP-NP.

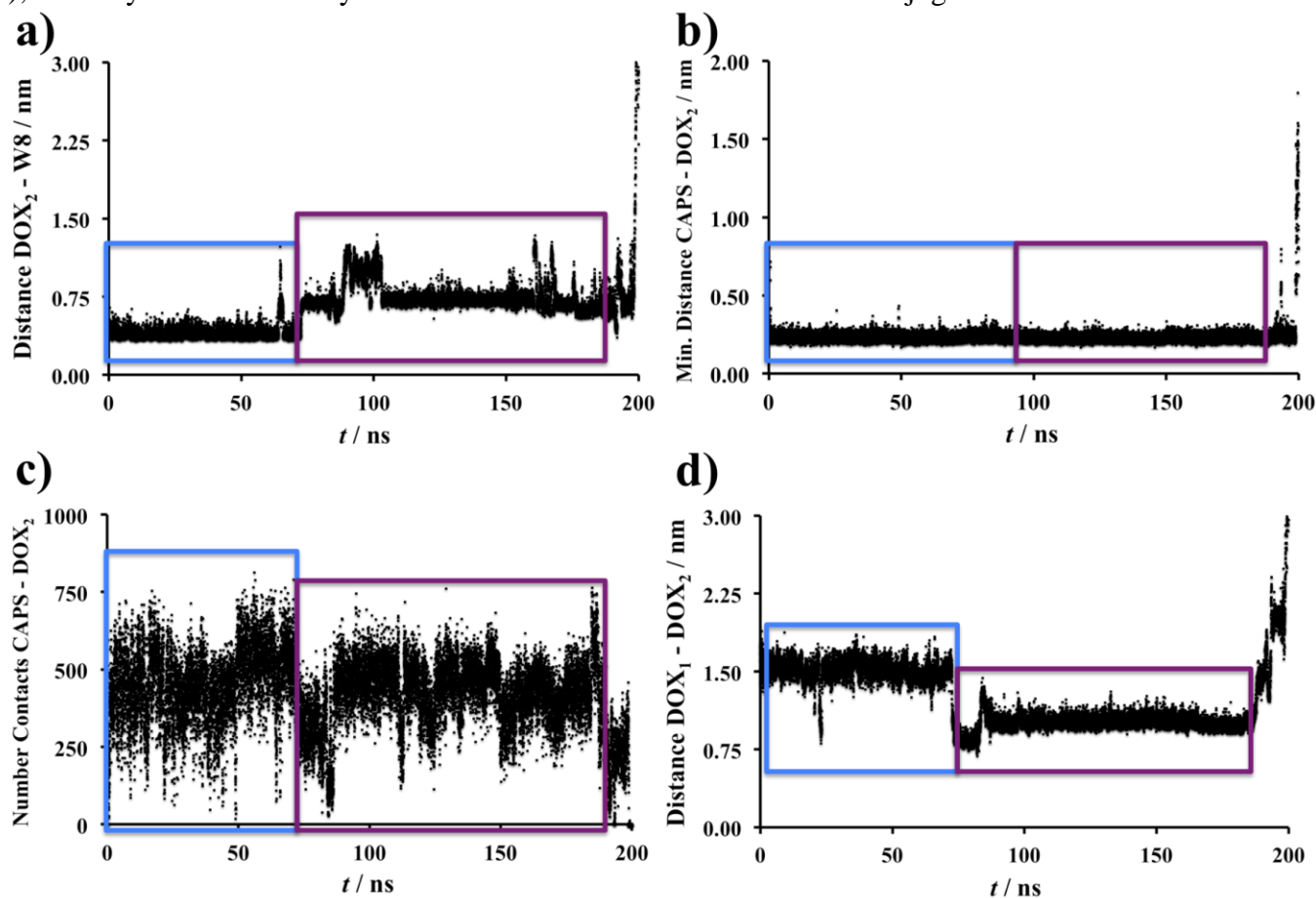


Figure S12. a) Distance between the COMs of the indole of W8 and the anthracycline part of DOX₂; b) minimum distance between the methyl thiolate caps and DOX₂; c) number of contacts between the methyl thiolate caps of the Au-NP and DOX₂; d) distance between the COMs of the anthracycline part of DOX₁ and DOX₂. Blue boxes mark the CAPS–DOX₂–W8 sandwich structure (**Figure S5**), violet boxes indicate the non-specific intercalation of DOX₂ in-between the caps of the NP and the backbone of the peptide (**Figure S6-S7**).

Table S4. Average values and standard deviations of the distances W8–DOX₂ and DOX₁–DOX₂, minimum distance between the methyl thiolate caps and DOX₂, and number of contacts between the methyl thiolate caps and DOX₂; separate estimates are compiled for the CAPS–DOX₂–W8 configuration and the non-specific intercalation of DOX₂ in-between the caps and the backbone of the peptide.

Adsorption configuration	CAPS–DOX ₂ –W8	CAPS–DOX ₂ –peptide
Distance (W8–DOX ₂) / nm	0.41 ± 0.06	0.75 ± 0.14
Minimum Distance (CAPS–DOX ₂) / nm	0.24 ± 0.02	0.24 ± 0.02
Number of Contacts (CAPS–DOX ₂)	451 ± 120	422 ± 100
Distance (DOX ₁ –DOX ₂) / nm	1.51 ± 0.11	1.02 ± 0.11

The adsorption configurations of DOX₂ at $t > 185$ ns (**Figure S8-S9**) are relatively short living (about 5 ns), and, thus, are not further quantified statistically. The dissociation of the drug from the DDS component at $t > 195$ ns directly becomes visible by the increasing distances DOX₂–W8, DOX₂–CAPS, and DOX₁–DOX₂ (**Figure S12a-b,d**), as well as by the reduced number of contacts between DOX₂ and the caps of the NP (**Figure S12c**).

4 Analysis of the MD trajectories at higher pH

In this section, we discuss the performed MD simulations for the associate NP-DBP-2DOX at higher pH values (see main manuscript). The DDS component NP-DBP-2DOX possesses three positive charges: two of them are carried by the amine function of the two DOX molecules, and one refers to the cysteine residue in the DBP. If the pH is increased, these three entities may be deprotonated, and thus lose their positive charge. The different charging of the associate NP-DBP-2DOX could alter the electrostatics in the system and, hence, affect the intermolecular interactions between the molecules in the model. To mimic pH values referring to alkaline conditions, e.g. such as those in the gastrointestinal tract, we have modeled the component NP-DBP-2DOX as a neutral system. In addition, three chloride counterions were removed, while all other parameters of the simulation, including the lengths of the various stages, were left the same as in the simulation with the charged molecules.

Equilibration of the (uncharged) associate NP-DBP-2DOX is verified by the evolution of the total energy, temperature, pressure, and the root-mean-square deviation (RMSD) of the atomic coordinates of the highly flexible DBP with respect to the coordinates of the minimized structure. A summary is given in **Figure S13**, while the average values are collected in **Table S5**.

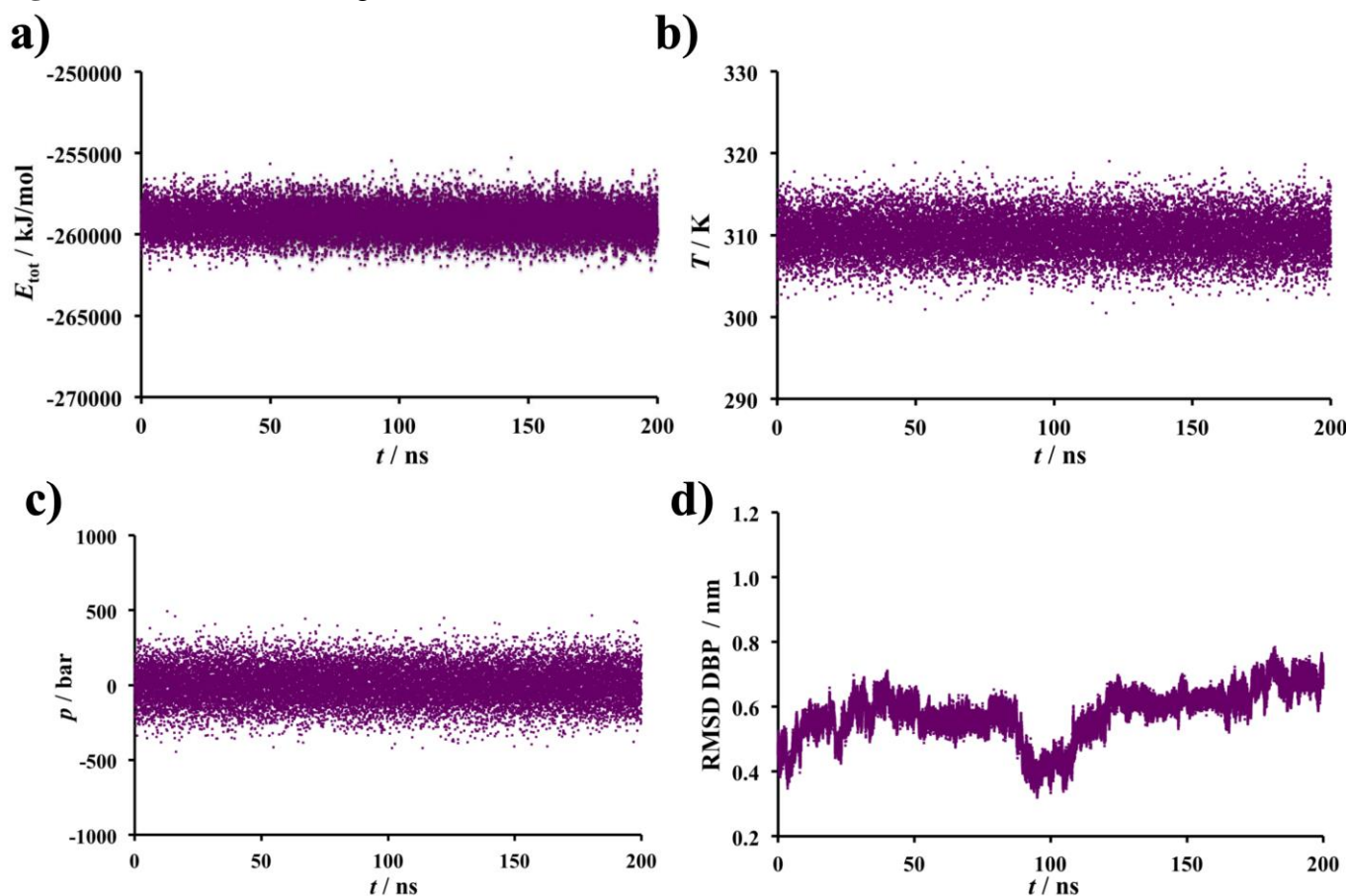


Figure S13. a) Total energy, b) temperature, c) pressure, and d) RMSD of the DBP in the uncharged associate NP-DBP-2DOX during the production phase.

Table S5. Average values and standard deviations of total energy, temperature, and pressure for the uncharged associate NP-DBP-2DOX within the production phase (200 ns).

System	E_{tot} / kJ/mol	T / K	p / bar
NP-DBP-2DOX	-259146 ± 917	310.0 ± 2.4	1.0 ± 119.7

To allow comparison of the uncharged associate NP-DBP-2DOX to the simulations reported in Section 3, we have chosen the same starting configuration for the MD simulations, that is, DOX₁ is stabilized by the tryptophan residue W5 and the caps of the Au-NP, while DOX₂ is placed randomly in the saline solution. Already during relaxation of the entire system, DOX₂ also adsorbs on the NP-DBP carrier and different adsorption sites for this drug entity are witnessed. The surface chemistry of the two drug molecules is discussed in the following.

In section 3, it was explained that two different adsorption states are observed for DOX₁: it is either intercalated between the caps of the NP and W5 (**Figures S5 – S6**) or stacked by W5 in a perpendicular orientation to the NP surface (**Figures S7 – S9**). For the uncharged associate NP-DBP-2DOX, the latter adsorption configuration is not witnessed. Throughout the entire production phase of 200 ns, DOX₁ is stabilized in a sandwich-like configuration between the caps of the NP and W5. Yet, it is possible to recognize that there are two patterns for the CAPS – DOX₁ – W5 adsorption state, namely, one configuration with smaller distance between DOX₁ and W5 (observed for $0 \text{ ns} < t < 16 \text{ ns}$ and $88 \text{ ns} < t < 108 \text{ ns}$) and one state with a somewhat larger DOX₁ – W5 distance (observed for $16 \text{ ns} < t < 88 \text{ ns}$ and $108 \text{ ns} < t < 200 \text{ ns}$; **Figure S14a**). These different configurations are a result of the fact that the indole of W5 can either interact with the anthracycline part of DOX₁ (small distance) or the sugar residue of DOX₁ (large distance). If the indole of W5 interacts with the anthracycline part of DOX₁, the minimum distance of DOX₁ to the caps of the NP is slightly larger (**Figure S14b**), which is accompanied with a reduced number of contacts between DOX₁ and the caps of the NP (**Figure S14c**). While the change in adsorption configuration for DOX₁ in the associate NP-DBP-2DOX from intercalated to stacked in a perpendicular orientation was traced to the location of the tryptophan residue W8 (**Figure S11d**), this finding does not hold true for the uncharged associate NP-DBP-2DOX (**Figure S14d**). Rather, the adsorption states of DOX₁ are independent of W8. This outcome can also be related to the fact that W8 is engaged in the stabilization of the second DOX entity (*vide infra*). Average data for the two adsorption configurations CAPS – DOX₁ – W5 are summarized in **Table S6**.

Table S6. Average values and standard deviations of the distances W5–DOX₁ and W8–DOX₁, minimum distance between the methyl thiolate caps and DOX₁, and number of contacts between the methyl thiolate caps and DOX₁; separate estimates are compiled for the two CAPS– DOX₁–W5 configurations in that the indole of W5 interacts either with the anthracycline fragment or with the sugar residue of DOX₁.

Adsorption configuration	CAPS–DOX ₁ –W5 (anthracycline - indole)	CAPS–DOX ₁ –W5 (sugar - indole)
Distance (W5–DOX ₁) / nm	0.38 ± 0.06	0.59 ± 0.04
Minimum distance (CAPS–DOX ₁) / nm	0.27 ± 0.06	0.24 ± 0.02
Number of contacts (CAPS– DOX ₁)	185 ± 97	393 ± 103
Distance (W8–DOX ₁) / nm	1.17 ± 0.19	1.07 ± 0.25

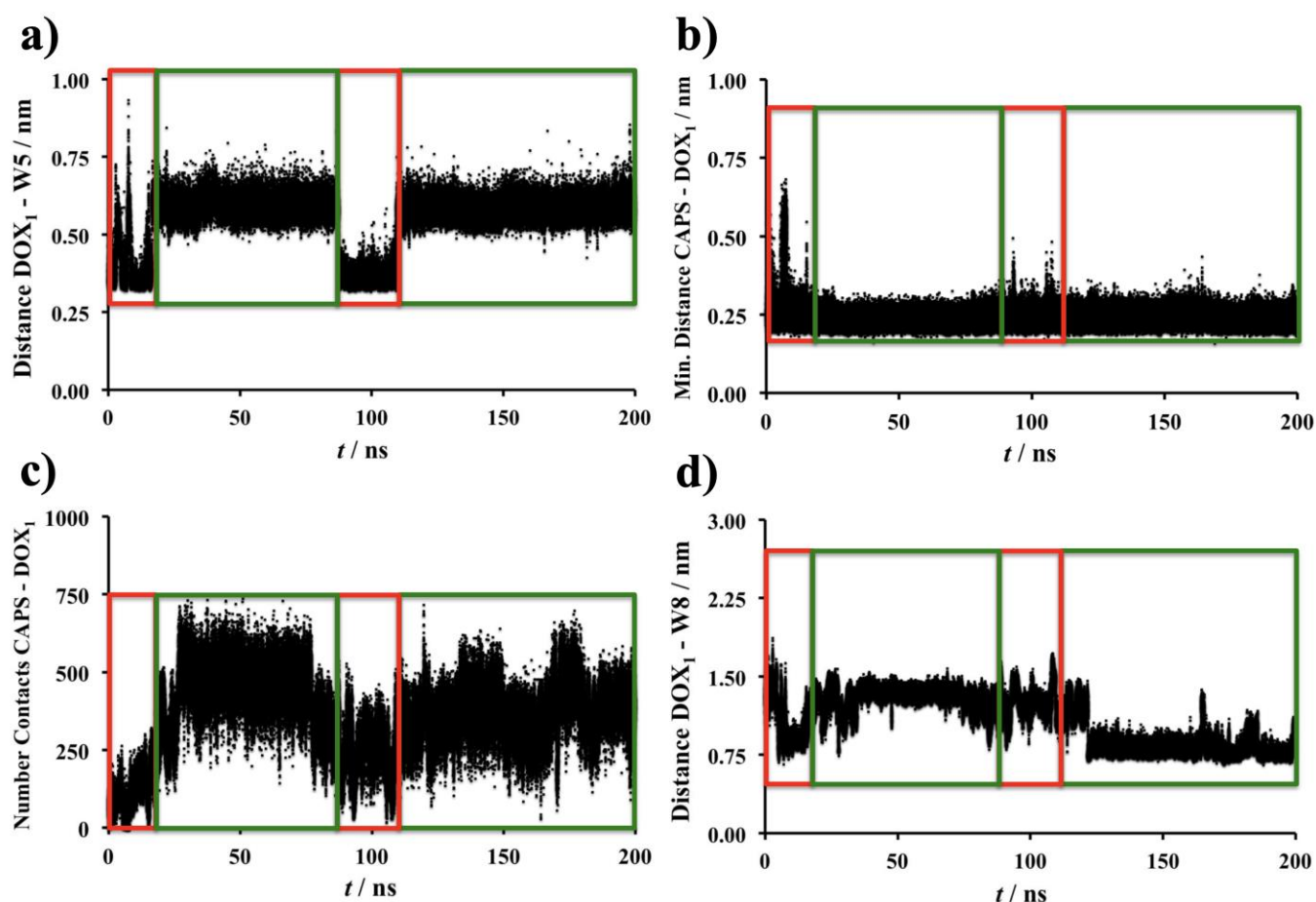


Figure S14. **a)** Distance between the COMs of the indole of W5 and the anthracycline part of DOX₁; **b)** minimum distance between the methyl thiolate caps and DOX₁; **c)** number of contacts between the methyl thiolate caps of the Au-NP and DOX₁; **d)** distance between the COMs of the indole of W8 and the anthracycline part of DOX₁. Red and green boxes mark the CAPS–DOX₁–W5 sandwich structures in which the indole of W5 interacts either with the anthracycline or sugar part of DOX₁, respectively.

The surface chemistry of DOX₂ is similar relating to the number of adsorption configurations observed, yet essentially different to the observations made in section 3 for the charged associate NP-DBP-2DOX. At the beginning of the trajectory, DOX₂ interacts with the tyrosine residue Y9. It is worth recalling that the interaction of DOX₂ with Y9 is repulsive for the charged associate NP-DBP-2DOX (**Figure S9 – S10**), whereas for the uncharged DDS component DOX₂ does not desorb from this residue. Yet, the interaction of DOX₂ with Y9 is short-term ($0 \text{ ns} < t < 24 \text{ ns}$; **Figure S15a**), and DOX₂ is stacked by the tryptophan residue W13 afterwards ($24 \text{ ns} < t < 135 \text{ ns}$; **Figure S15b**). This finding is fundamentally different to the charged associate NP-DBP-2DOX because a direct interaction of DOX₂ and W13 is not observed. Obviously, the altered electrostatics due to the removal of three protons (*vide supra*) enables both DOX₁ and DOX₂ to be stacked in sandwich-like configurations between the tryptophan residues W5 or W13 and the caps of the NP. The existence time of this configuration amounts to 111 ns, which excels the longest-living adsorption state of the charged associate NP-DBP-2DOX (**Figure 3**). For $135 \text{ ns} < t < 164 \text{ ns}$, DOX₂ is non-specifically intercalated between the caps of the NP and the peptide backbone. This adsorption state was also observed for the charged associate NP-DBP-2DOX (**Figure S6 – S7**). At the end of the trajectory, $164 \text{ ns} < t < 200 \text{ ns}$, DOX₂ is stacked in a sandwich-like configuration between the tryptophan residues W8 and W13 (**Figure S15b-c**), thereby still maintaining contact with the caps of the NP through its sugar residue (**Figure S15d**). Average data for the various adsorption configurations of DOX₂ are summarized in **Table S7**.

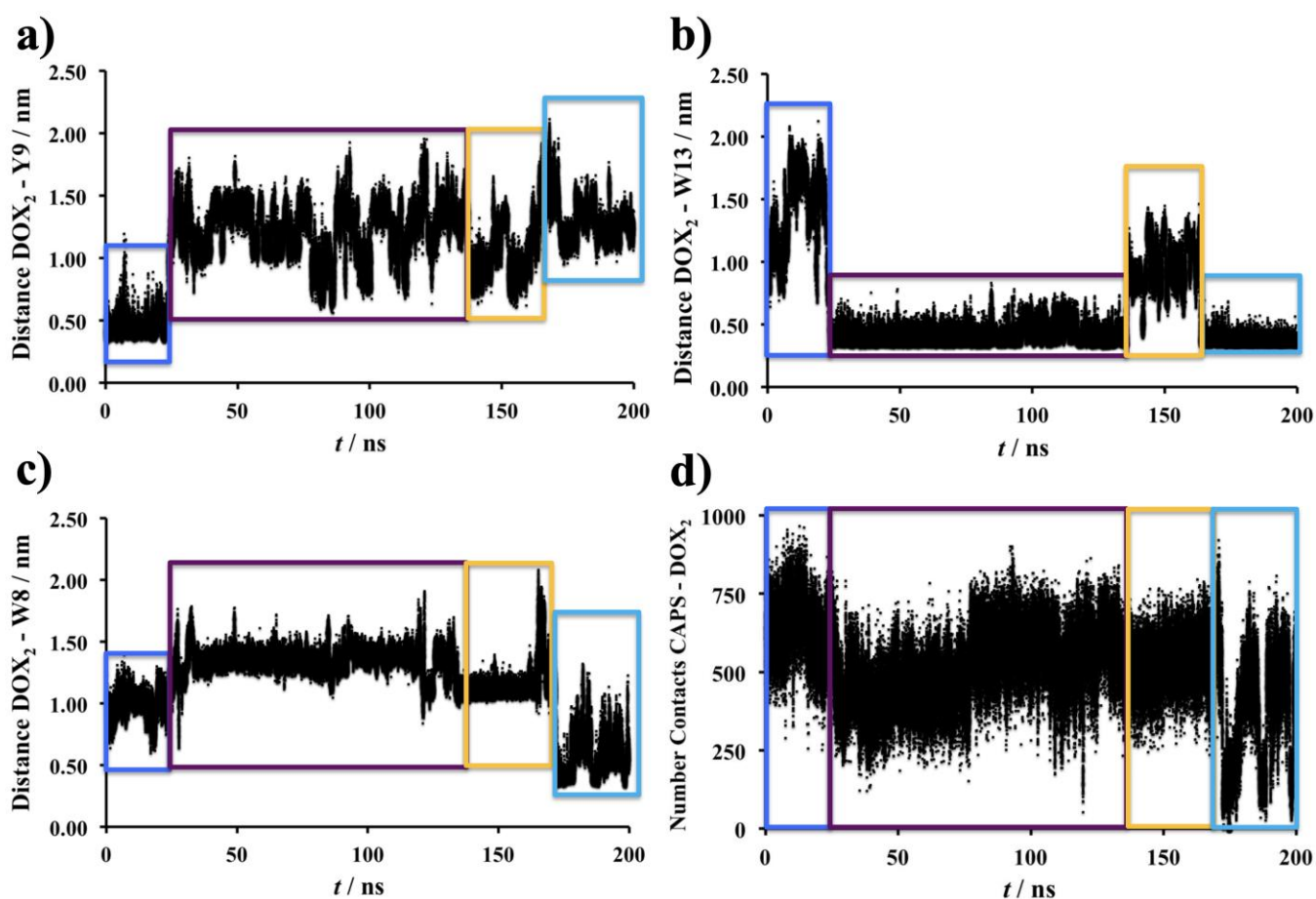


Figure S15. a) Distance between the COMs of the aromatic ring of Y9 and the anthracycline part of DOX₂; b) distance between the COMs of the indole of W13 and the anthracycline part of DOX₂; c) distance between the COMs of the indole of W8 and the anthracycline part of DOX₂; d) number of contacts between the methyl thiolate caps of the Au-NP and DOX₂. Blue boxes mark the CAPS–DOX₂–Y9 sandwich structure, violet boxes indicate the CAPS–DOX₂–W13 sandwich structure, orange boxes mark the non-specific intercalation of DOX₂ between the caps of the NP and the DBP, and turquoise boxes denote the sandwich configuration W8–DOX₂–W13.

Table S7. Average values and standard deviations of the distances Y9–DOX₂, W13–DOX₂, and W8–DOX₂, and number of contacts between the methyl thiolate caps and DOX₂; separate estimates are compiled for the four different adsorption states of DOX₂ (**Figure S15**).

Adsorption configuration	CAPS– DOX ₂ –Y9	CAPS– DOX ₂ –W13	CAPS–DOX ₂ – peptide	W8–DOX ₂ – W13
Distance (Y9–DOX ₂) / nm	0.47 ± 0.11	1.23 ± 0.20	1.06 ± 0.20	1.32 ± 0.17
Distance (W13–DOX ₂) / nm	1.35 ± 0.36	0.41 ± 0.07	0.93 ± 0.22	0.37 ± 0.03
Distance (W8–DOX ₂) / nm	0.99 ± 0.10	1.35 ± 0.10	1.12 ± 0.04	0.74 ± 0.37
Number of contacts (CAPS– DOX ₂)	642 ± 92	512 ± 111	527 ± 76	404 ± 177

In summary, our MD simulations for the uncharged associate NP-DBP-2DOX indicate that DOX₁ has a stable adsorption site, namely W5, throughout the entire simulation time of 200 ns. This finding is in accordance with the trajectories for the charged associate NP-DBP-2DOX (Section 3 above) and the simulations for one drug entity in the unit cell.^[S1] However, for the uncharged associate NP-DBP-2DOX the adsorption state of DOX₁ is decoupled from the location of the tryptophan residue W8 (**Figure S14d**), which differs to the results obtained for the charged component NP-DBP-2DOX (**Figure S11d**) or for that with one drug entity in the unit cell.^[S1] Decoupling the adsorption state of DOX₁ from the location of W8 has a beneficial effect for the entire DDS component because it allows DOX₂ to intercalate between the caps of the NP and W13 or to form a sandwich with W8 and W13 (**Figure S15**). Both adsorption

states, which reveal existence times that exceed the adsorption configurations for the charged associate NP-DBP-2DOX (**Figure 3**), are not present for the charged system (**Figures S5 – S10**); yet, interaction of DOX with W8 and/or W13 has been reported for MD simulations without presence of the Au-NP as a carrier moiety.^[S2] Therefore, it can be concluded in an impartial fashion that the pH of the medium is a parameter to be tuned for an improved stabilization of anthracycline drugs within DDS components. Considering that DOX₂ does not desorb from the uncharged associate NP-DBP-2DOX during the entire simulation time, as lower proton activities are beneficial to the associate NP-DBP-2DOX for drug delivery, an oral uptake of the chemotherapeutic agent and its carriers could be suggested.

References

- [S1] Exner, K.S.; Ivanova, A. Identifying a gold nanoparticle as a proactive carrier for transport of a doxorubicin-peptide complex. *Coll. Surf. B* **2020**, *194*, 111155.
- [S2] Gocheva, G.; Peneva, K.; Ivanova, A. Self-assembly of doxorubicin and a drug-binding peptide studied by molecular dynamics. *Chem. Phys.* **2019**, *525*, 110380.